SUPPLEMENTAL INFORMATION INVENTORY

- Fig S1 and legend-Related to Fig 1
- Fig S2 and legend-Related to Fig 2
- Fig S3 and legend-Related to Fig 3
- Fig S4 and legend-Related to Fig 3 & 4
- Fig S5 and legend-Related to Fig 7
- Supplemental Table S1-Related to Fig 1
- Supplemental Experimental Procedures and Supplemental References

Figure S1

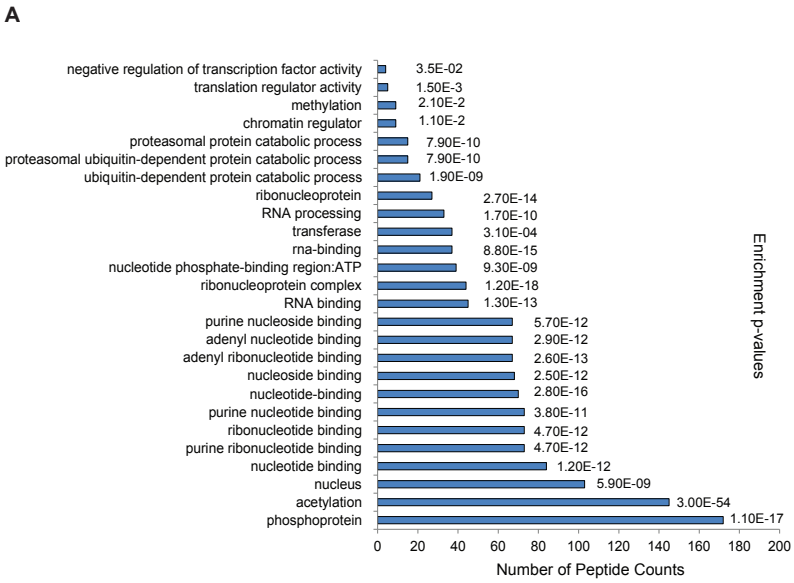
A
negative regulation of transcription factor activity
translation regulator activity
methylation
chromatin regulator
proteasomal protein catabolic process
proteasomal ubiquitin-dependent protein catabolic process
ubiquitin-dependent protein catabolic process
ribonucleoprotein
RNA processing
transferase
rna-binding
nucleotide phosphate-binding region:ATP
ribonucleoprotein complex
RNA binding
purine nucleoside binding
adenyl nucleotide binding
adenyl ribonucleotide binding
nucleoside binding
nucleotide-binding
purine nucleotide binding
ribonucleotide binding
purine ribonucleotide binding
nucleotide binding
nucleus
acetylation
phosphoprotein
3.5E-02
1.50E-3
2.10E-2
1.10E-2
7.90E-10
7.90E-10
1.90E-09
2.70E-14
1.70E-10
3.10E-04
8.80E-15
9.30E-09
1.20E-18
1.30E-13
5.70E-12
2.90E-12
2.60E-13
2.50E-12
2.80E-16
3.80E-11
4.70E-12
4.70E-12
1.20E-12
5.90E-09
3.00E-54
1.10E-17
0 20 40 60 80 100 120 140 160 180 200
Number of Peptide Counts
Enrichment p-values

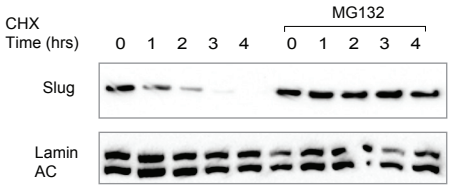
B
CHX
Time (hrs)
0 1 2 3 4
MG132
0 1 2 3 4
Slug
Lamin
AC

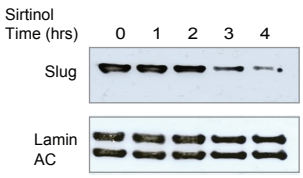
C
Sirtinol
Time (hrs)
0 1 2 3 4
Slug
Lamin
AC

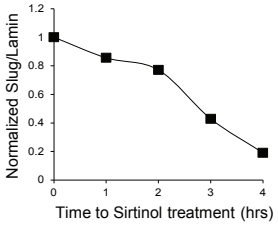
Normalized Slug/Lamin
Time to Sirtinol treatment (hrs)

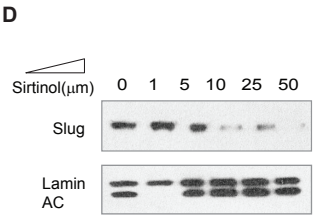
D
Sirtinol(μm)
0 1 5 10 25 50
Slug
Lamin
AC

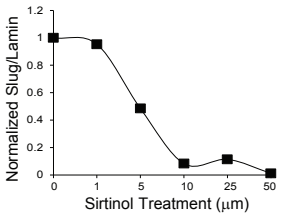
Normalized Slug/Lamin
Sirtinol Treatment (μm)

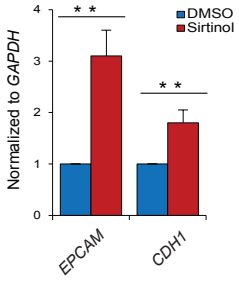
E
DMSO
Sirtinol
Normalized to GAPDH
EPCAM
CDH1

Figure S1. Inhibition of protein acetylation modulates Slug protein abundance (Related to Figure 1).

(A) Analysis of Slug-interacting proteins identified from proteomic SLUG coIP/MS. Shown is a list of associated molecular functions from the DAVID functional annotation tool. False discovery rates are shown as Benjamini-Hochberg p-values.

(B) MCF10A cells were treated with cycloheximide (CHX) to prevent *de novo* protein synthesis, in the presence or absence of proteasomal inhibitor MG132, at indicated time intervals. Immunoblots of Slug and Lamin A/C protein levels at the indicated time intervals.

(C) (Left) Immunoblots showing Slug and Lamin A/C protein levels at the indicated time intervals. MCF10A cells were treated with 25 μm of Sirtinol. (Right) Quantification of relative Slug protein levels normalized to Lamin A/C.

(D) (Left) Immunoblots showing Slug and Lamin A/C protein levels with increasing concentrations of sirtinol. MCF10A cells were treated for 4 hours. (Right) Quantification of relative Slug protein levels normalized to Lamin A/C.

(E) Expression of Slug target genes *EPCAM* and *CDH1* in MCF10A cells after 4 hours of sirtinol treatment (25 μm). Data are shown as mean ± SEM (n = 3), * * $p < 0.01$.

Figure S2

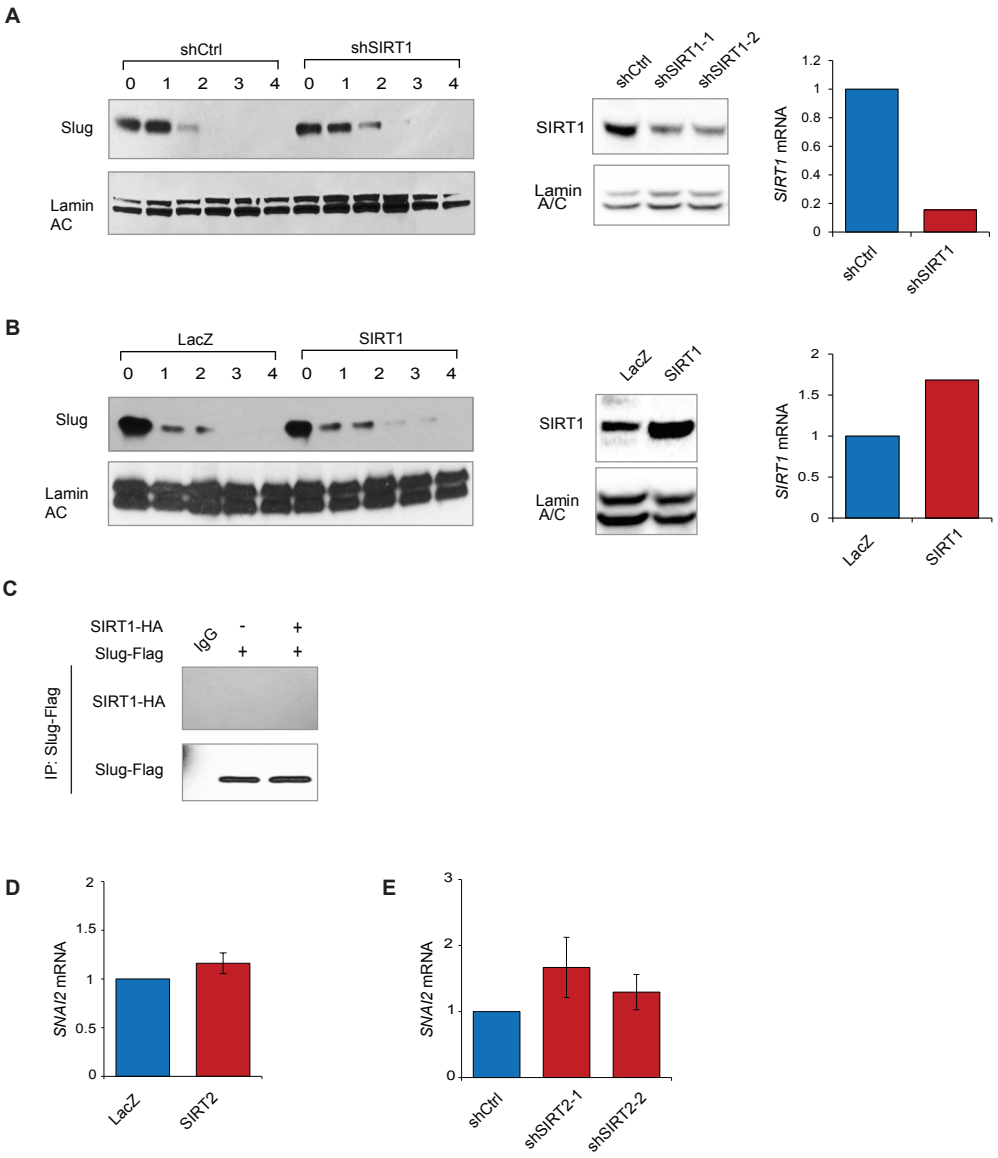
A
shCtrl
shSIRT1
0 1 2 3 4 0 1 2 3 4
Slug
Lamin AC
shCtrl
shSIRT1-1
shSIRT1-2
SIRT1
Lamin A/C
SIRT1 mRNA
1.2
1
0.8
0.6
0.4
0.2
0
shCtrl
shSIRT1
B
LacZ
SIRT1
0 1 2 3 4 0 1 2 3 4
Slug
Lamin AC
LacZ
SIRT1
SIRT1
Lamin A/C
SIRT1 mRNA
2
1.5
1
0.5
0
LacZ
SIRT1
C
SIRT1-HA
IgG - +
Slug-Flag + +
IP: Slug-Flag
SIRT1-HA
Slug-Flag
D
SNAI2 mRNA
2
1.5
1
0.5
0
LacZ
SIRT2
E
SNAI2 mRNA
3
2
1
0
shCtrl
shSIRT2-1
shSIRT2-2

Figure S2. Genetic manipulation of SIRT1 does not affect Slug protein abundance (Related to Figure 2)

(A) (Left) Immunoblots showing levels of Slug and Lamin A/C in CHX-treated MCF10A cells overexpressing either shSIRT1 or a non-silencing shRNA control (shCtrl). (Right) SIRT1 protein level is assessed by immunoblot, and *SIRT1* transcript expression is assessed by qRT-PCR

(B) (Left) Immunoblots showing levels of Slug and Lamin A/C in CHX-treated MCF10A cells overexpressing SIRT1 or LacZ control. (Right) SIRT1 protein level is assessed by immunoblot, and *SIRT1* transcript expression is assessed by qRT-PCR.

(C) Lysates from HEK293T cells transfected with HA-tagged SIRT1 (SIRT1-HA) and Flag-tagged Slug (Flag-Slug) were subjected anti-Flag immunoprecipiation. Immunoblots of Flag-Slug and SIRT1-HA are shown.

(D) *SNAI2* transcript expression in MCF10A cells overexpressing SIRT2 or LacZ (n = 3) as determined by qRT-PCR. Data are shown as mean ± SEM.

(E) *SNAI2* transcript expression in MCF10A cells expressing shSIRT2 or shCtrl (n = 3) as determined by qRT-PCR. Data are shown as mean ± SEM.

Figure S3

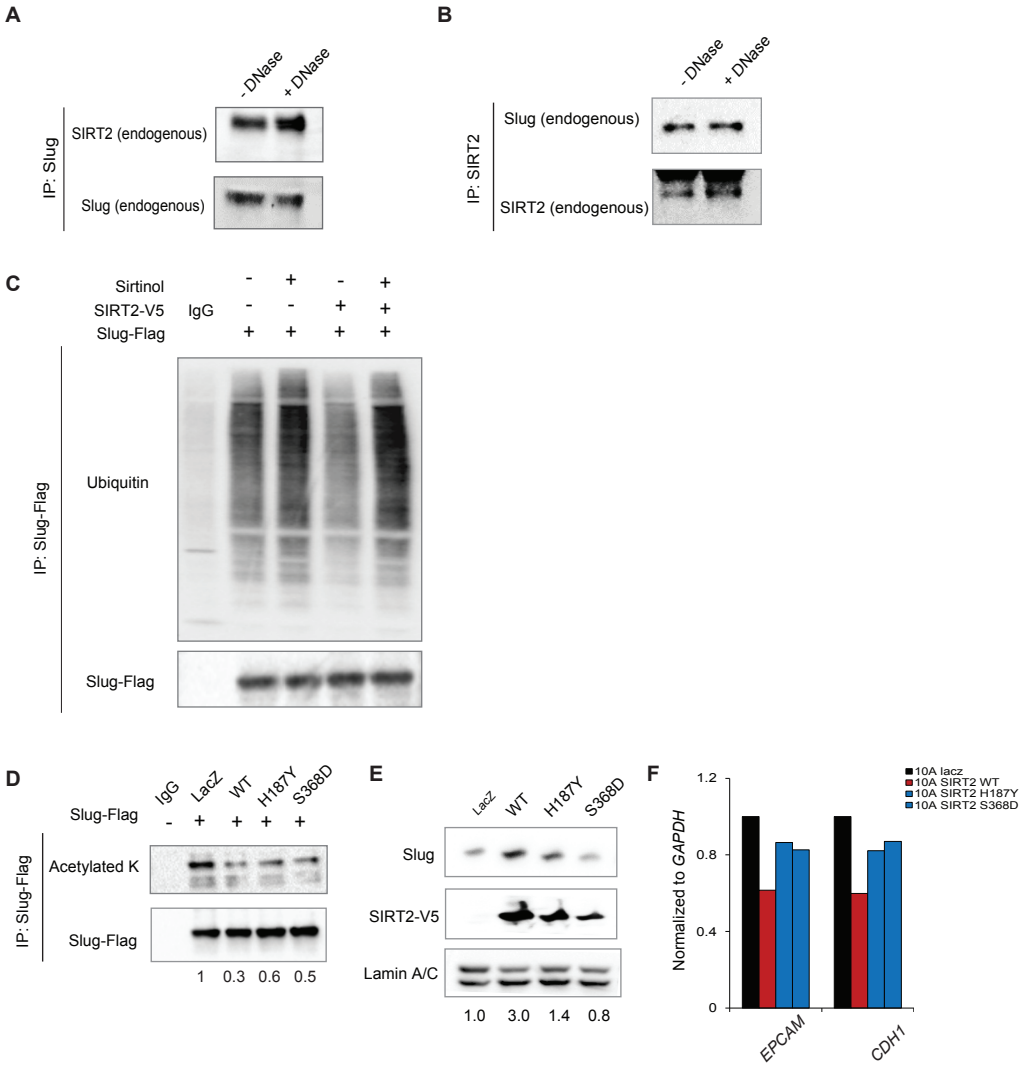
A
- DNase
+ DNase
IP: Slug
SIRT2 (endogenous)
Slug (endogenous)
B
- DNase
+ DNase
IP: SIRT2
Slug (endogenous)
SIRT2 (endogenous)
C
Sirtinol
SIRT2-V5
IgG
Slug-Flag
IP: Slug-Flag
Ubiquitin
Slug-Flag
D
IgG
LacZ
WT
H187Y
S368D
Slug-Flag
IP: Slug-Flag
Acetylated K
Slug-Flag
1 0.3 0.6 0.5
E
LacZ
WT
H187Y
S368D
Slug
SIRT2-V5
Lamin A/C
1.0 3.0 1.4 0.8
F
10A lacz
10A SIRT2 WT
10A SIRT2 H187Y
10A SIRT2 S368D
Normalized to GAPDH
1.2
0.8
0.4
0
EPCAM
CDH1

Figure S3. Data related to Figure 3.

(A) Lysates from MCF10A were subjected to anti-Slug immunoprecipitation (A) and anti-SIRT2 immunoprecipitation (B) in the presence or absence of *DNase*. Immunoblots of endogenous Slug and SIRT2 are shown.

(C) Immunoblots of ubiquitin and Flag-Slug from anti-Flag immunoprecipitation of HEK293T cells co-overexpressing Flag-Slug, wild-type SIRT2 (WT) or LacZ control, in the presence or absence of sirtinol.

(D) Immunoblots of pan-acetylated lysine and Flag-Slug from anti-Flag immunoprecipitation of HEK293T cells co-overexpressing Flag-Slug and either wild-type SIRT2, catalytically inactive SIRT2 mutants H187Y or S368D, or control LacZ. Relative levels of acetylated Slug protein were quantified and are shown below the immunoblots.

(E) Immunoblots showing levels of Slug, SIRT2-V5 and Lamin A/C in MCF10A cells transfected with wild-type SIRT2 (WT), catalytically inactive SIRT2 mutants (H187Y and S368D) or control LacZ. Relative levels of Slug protein were quantified and are shown below the immunoblots.

(F) Expression of Slug target genes *EPCAM and CDH1* in MCF10A cells transfected with wild-type SIRT2 (WT), catalytically inactive SIRT2 mutants (H187Y and S368D) or control LacZ.

Figure S4

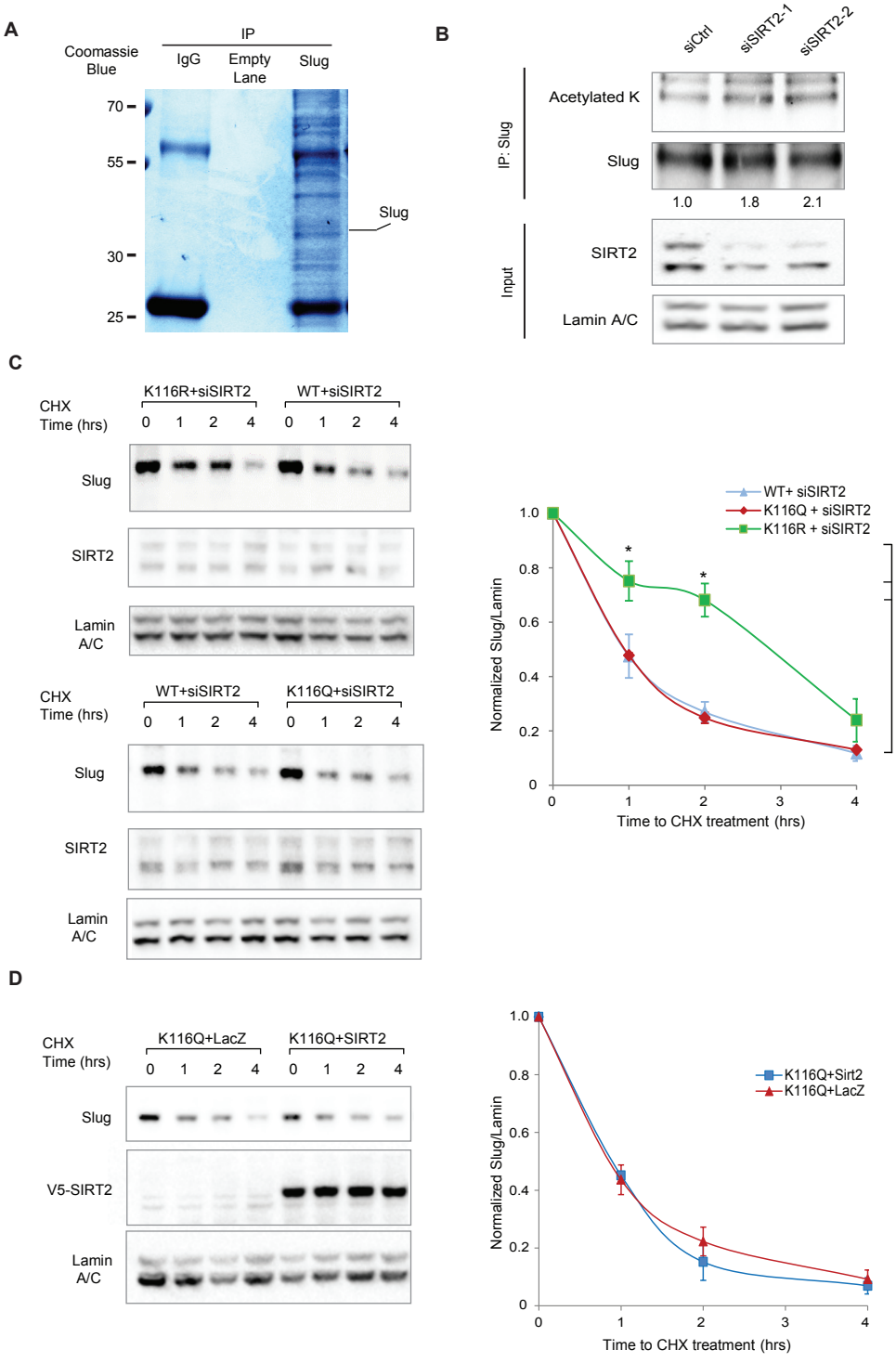
A
IP
Coomassie Blue
IgG
Empty Lane
Slug
70
55
30
25
Slug
B
siCtrl
siSIRT2-1
siSIRT2-2
IP: Slug
Acetylated K
Slug
1.0
1.8
2.1
Input
SIRT2
Lamin A/C
C
K116R+siSIRT2
WT+siSIRT2
CHX Time (hrs)
0 1 2 4 0 1 2 4
Slug
SIRT2
Lamin A/C
WT+siSIRT2
K116Q+siSIRT2
CHX Time (hrs)
0 1 2 4 0 1 2 4
Slug
SIRT2
Lamin A/C
WT+ siSIRT2
K116Q + siSIRT2
K116R + siSIRT2
Normalized Slug/Lamin
Time to CHX treatment (hrs)
*
*
D
K116Q+LacZ
K116Q+SIRT2
CHX Time (hrs)
0 1 2 4 0 1 2 4
Slug
V5-SIRT2
Lamin A/C
K116Q+Sirt2
K116Q+LacZ
Normalized Slug/Lamin
Time to CHX treatment (hrs)

Figure S4. SIRT2 catalytic function is necessary for Slug protein regulation (Related to Figures 3 and 4)

(A) Coomassie staining of FLAG immunoprecipitated HEK293T cells lysates overexpressing FLAG-Slug. Arrow indicates a band with the approximate molecular weight of Slug protein, which was digested, analyzed and confirmed by mass-spectrometry.

(B) (Left) Immunoblots of pan-acetylated lysine and Slug from anti-Slug immunoprecipitation of MCF10A cells co-expressing either siSIRT2 or a non-silencing siRNA control (siCtrl), and Slug. Relative levels of acetylated Slug protein were quantified and are shown below the immunoblots.

(C) (Top left) Immunoblots comparing the effect of SIRT2 knockdown on wild-type (WT) Slug versus non-acetyl-lysine-mimic K116R Slug mutant in MCF10A cells. (Bottom left) Immunoblots comparing the effect of SIRT2 knockdown on wild-type (WT) Slug versus acetyl-lysine-mimic K116Q Slug mutant in MCF10A cells. (Right) The degradation curves of relative Slug protein from three independent experiments are normalized to Lamin A/C and plotted for cells overexpressing WT Slug + siSIRT2 (blue), K116Q + siSIRT2 (red), and K116R Slug mutant + siSIRT2 (green). Data shown are mean ± SEM, * $p < 0.05$.

(D) (Left) Immunoblots showing the stability of the acetylation-mimic K116Q Slug mutant in cells overexpressing either the LacZ control or SIRT2. Immunoblot of V5-SIRT2 is included to show SIRT2 overexpression. (Right) The degradation curves of relative Slug protein from three independent experiments are normalized to Lamin A/C and plotted for cells overexpressing SIRT2 (blue) and LacZ (red). Data shown are mean ± SEM, * $p < 0.05$.

Figure S5

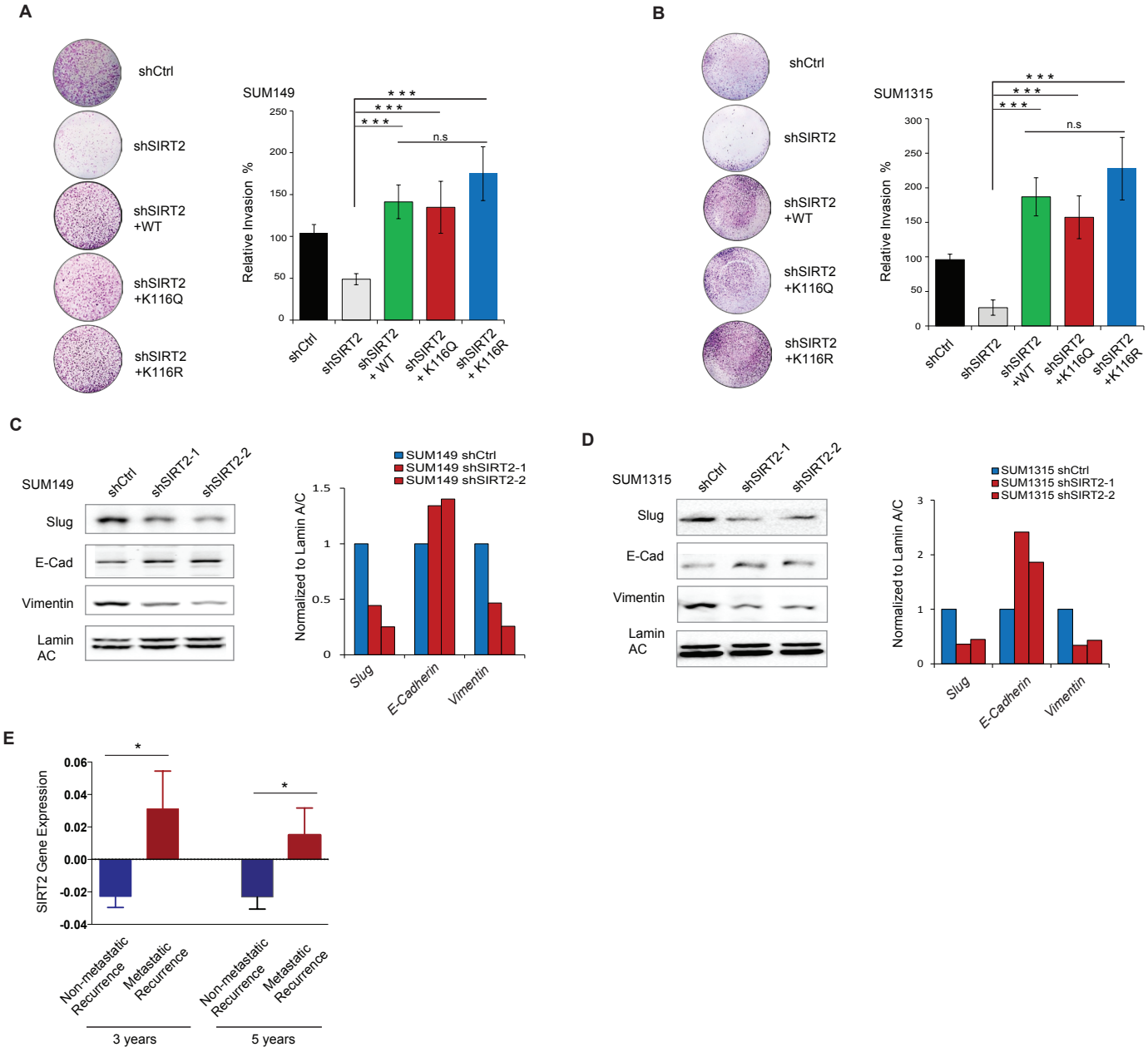
A
shCtrl
shSIRT2
shSIRT2 +WT
shSIRT2 +K116Q
shSIRT2 +K116R
SUM149
Relative Invasion %
n.s
B
SUM1315
C
SUM149
shCtrl
shSIRT2-1
shSIRT2-2
Slug
E-Cad
Vimentin
Lamin AC
SUM149 shCtrl
SUM149 shSIRT2-1
SUM149 shSIRT2-2
Normalized to Lamin A/C
Slug
E-Cadherin
Vimentin
D
SUM1315
SUM1315 shCtrl
SUM1315 shSIRT2-1
SUM1315 shSIRT2-2
E
SIRT2 Gene Expression
Non-metastatic Recurrence
Metastatic Recurrence
3 years
5 years

Figure S5. Data related to Figure 7

(A) (Left) Representative images showing the effect of overexpressing wild-type, the non-acetyl-lysine mimic (K116R) or the acetyl-lysine mimic (K116Q) version of Slug on the invasive capacity of SIRT2-depleted SUM149 cancer cells, compared to non-targeting hairpin control (shCtrl). (Right) The total number of cells invading through the Matrigel coated transwell were quantified (n = 3 per cell line). Data are shown as mean ± SEM. *** $p < 0.001$

(B) (Left) Representative images showing the effect of overexpressing wild-type, the non-acetyl-lysine mimic (K116R) or the acetyl-lysine mimic (K116Q) version of Slug on the invasive capacity of SIRT2-depleted SUM1315 cancer cells, compared to non-targeting hairpin control (shCtrl). (Right) The total number of cells invading through the Matrigel coated transwell were quantified (n = 3 per cell line). Data are shown as mean ± SEM. *** $p < 0.001$

(C) (Left) Immunoblots showing the effect of SIRT2 depletion on Slug, E-Cadherin and vimentin protein levels, compared to non-targeting hairpin control (shCtrl) in SUM149 basal-like breast cancer cells. (Right) Quantification of Slug, E-Cadherin and vimentin protein levels normalized to Lamin A/C.

(D) (Left) Immunoblots showing the effect of SIRT2 depletion on Slug, E-Cadherin and vimentin protein levels, compared to non-targeting hairpin control (shCtrl) in SUM1315 BLBC cells. (Right) Quantification of Slug, E-Cadherin and vimentin protein levels normalized to Lamin A/C.

(E) Comparison of *SIRT2* expression (as $\log_2$ fold change) between breast cancer patients presenting with or without metastatic recurrence at 3 years and 5 years reported in (van ’t Veer et al., 2002) . Data were analyzed using one-way ANOVA, Data shown are mean ± SEM, *$p<0.05$

SUPPLEMENTAL EXPERIMENTAL PROCEDURES

Cell lines and Tissue Culture

All cells were grown at 37°C with 5% CO_2. MCF10A cells were cultured in complete MEGM (Lonza) plus 100ng/ml cholera toxin. HEK293T cells were cultured in DMEM supplemented with 10% fetal bovine serum. SUM149 cells were cultured in Ham's F12 supplemented with 5 μg/ml insulin, 0.5 μg/ml hydrocortisone and 10% fetal bovine serum. SUM1315 cells were cultured in Ham's F12 supplemented with 5 μg/ml insulin, 20ng/ml EGF and 10% fetal bovine serum. Transfections were performed in serum-starved cells two hours prior to using FuGENE HD (Promega) according to the manufacturer's suggested protocol. For lentivirus production, HEK293T cells were co-transfected with pCMV-VSV-G, pCMV-ΔR8.2-Δvpr, and lentivirus expression vectors for 48 hours and viral supernatant were collected. For generation of stable cell lines, SUM149 and SUM1315 cells were incubated overnight in viral supernatant supplemented with 5 μg/ml protamine sulfate (Sigma) and subsequently selected by antibiotics.

Cloning and Plasmid Construction

pLKO.1-puro *SIRT2*-targeting shRNAs (TRCN0000040222 and TRCN0000040220) and *SIRT1*-targeting shRNAs (TRCN0000018979, TRCN0000018980) were purchased from Sigma-Aldrich. Donor vectors containing full-length *SIRT1, SIRT2* or *SNAI2* were cloned to pPGS-FLAG (Phillips et al., 2014) or plenti6.2-V5 (Life Technologies) tagged destination vectors as indicated. Site-directed mutagenesis was performed to generate point mutants of SIRT2 H187Y, SIRT2 S368D, Slug K8Q, Slug K116Q and Slug K116R. The mutagenic oligonucleotide primers used are listed below. PCR reactions for single amino acid mutations were run for 18 cycles of 50s at 95°C, 50s at 55°C, followed by 7 or 9 min at 68 °C, using the high-fidelity KAPA HotStart PCR Kit (KAPA Biosystems). The resulting mutant plasmids were verified by DNA sequencing.

Immunofluorescence and Immunohistochemistry

For immunofluorescence, cultured cells seeded on coverslips were fixed in 4% paraformaldehyde, permeabilized in 0.1% Triton-X 100 in PBS, and then blocked in 3% normal goat serum in PBS for 1hr at room temperature prior to incubation with primary antibodies overnight. Alexa Fluor 488- and Alexa Fluor 546-conjugated secondary antibodies (Life Technologies) were applied for 1 hour to detect protein and counterstained with 1 μg/ml DAPI to visualize nuclei. Sample were mounted on glass slides with the SlowFade Antifade Kit (Life Technologies). For paraffin-embedded human tissues, samples were first de-paraffinized in xylenes and dehydrated sequentially in 100%, 95% and 70% graded ethanols, followed by heat-induced antigen retrieval in Tris-EDTA (10 mM Tris, pH 9.0 and 1 mM EDTA) at 100°C for 20 minutes. Tissue sections were washed in PBS, blocked with 1% normal horse serum and 5% bovine serum albumin in PBS for 1 hour, and then incubated with primary antibodies overnight. Biotinylated secondary antibody (Vector Lab) was applied for 30 minutes, washed in PBS three times, and developed using the Vectastain ABC and Impact Substrate Kits (Vector Lab) according to the manufacturer's instructions. Tissues were counterstained with Mayer's haematoxylin and mounted with coverslips. Immunofluorescence and immunohistochemistry images were captured using an Eclipse 80i microscope and SPOT image acquisition software (Micro Video Instruments). Quantification and analysis of SIRT2 IHC were performed at the Histology Core at Beth Israel Deaconess Medical Center. Antibodies used for these procedures are listed below.

TCGA Cancer Genomic Data Mining

All TCGA data was obtained from the TCGA breast cancer online portal (https://tcgadata.nci.nih.gov/docs/publications/brca_2012/) (Koboldt et al., 2012) . For intrinsic molecular subtype identification, we utilized the PAM50 subtype calls as provided in the TCGA

portal (TCGA, Nature 2012). For histological subtype identification, we utilized the invasive lobular carcinoma and the invasive ductal carcinoma calls, combined with PAM50 subtype when available (TCGA, Cell 2015). Putative copy-number alteration of *SIRT2* based on GISTIC 2.0 values (-2 = homozygous deletion, -1 = heterozygous deletion, 0 = neutral/no change, 1 = gain, 2 = high level amplification) (Cerami et al., 2012) were extracted and data were analyzed using two-tailed unpaired student's t-tests between each intrinsic molecular or histological subtypes of breast cancer. Relative *SIRT2* mRNA expression values based on z-scores using the default threshold (2 SDs from the mean) (Gao et al., 2013) were extracted and data were analyzed using one-way ANOVA across multiple intrinsic molecular or histological subtypes of breast cancer.

Antibodies Used in This Study

Antibody	Host	Ventor/Catalog Number	IB	IP	IF	IHC
Slug	Rabbit	Cell Signaling (9585)	x		x	x
Slug	Mouse	Cell Signaling (9589)		x		
SIRT2	Rabbit	Millipore (09-843)	x	x		
SIRT2	Rabbit	Sigma (HPA011165)				x
SIRT2	Mouse	Abnova (H00022933-M01)			x	
Flag	Rabbit	Cell Signaling (2044)	x	x		
V5	Mouse	Life Technology (R960-25)	x			
Ac-Tubulin	Mouse	Sigma (T6793)	x			
Cyclin D1	Mouse	cell Signaling (2926)	x			
b-Actin	Mouse	Abcam (ab6276)	x			
Acetylated lysine	Rabbit	Cell Signaling (9441)	x			
Ubiquitin	Rabbit	Cell Signaling (3933)	x			
Lamin A/C	Rabbit	Cell Signaling (2032)	x			
Normal IgG	Mouse	Santa Cruz (sc-2025)		x		
Normal IgG	Rabbit	Santa Cruz (sc-2027)		x		
mouse (HRP)	Goat	Cell Signaling (7074)	x			
rabbit (HRP)	Goat	Cell Signaling (7076)	x			
rabbit (biotin)	Goat	Vector (BA-1000)				x
Rabbit (Alexa 488-)	Goat	Life Technology (A110008)			x	
Mouse (Alexa 546-)	Goat	Life Technology (A110003)			x	

Primer Sequences Used for Site-Directed Mutagenesis

Mutant	Forward Primer	Reverse Primer
SIRT2 H187Y	GAGGACTTGGTGGAGGCGTACGGCACCTTCTACACATC	GATGTGTAGAAGGTGCCGTACGCCTCCACCAAGTCCTC
SIRT2 S368D	CCAGCACTTCAGCTGACCCCAAGAAGTCC	GGACTTCTTGGGGTCAGCTGAAGTGCTGG
SNAI2 K8Q	GCTCCTTCCTGGTCCAGAAGCATTTCAAC	GTTGAAATGCTTCTGGACCAGGAAGGAGC
SNAI2K116Q	GAGGAAAGACTACAGTCCCAGCTTTCAGACCCCCATGC	GCATGGGGGTCTGAAAGCTGGGACTGTAGTCTTTCCTC
SNAI2 K116R	GTAAATACTGTGACAGGGAATATGTGAGCCTG	CAGGCTCACATATTCCCTGTCACAGTATTTAC

Primer Sequences Used for Real-time PCR (qPCR)

Gene	Forward Primer	Reverse Primer
SNAI2	TGTGACAAGGAATATGTGAGCC	TGAGCCCTCAGATTTGACCTG
EPCAM	AATCGTCAATGCCAGTGTACTT	TCTCATCGCAGTCAGGATCATAA
CDH1	GAACGCATTGCCACATACAC	GAATTCGGGCTTGTTGTCAT
SMA	CAGGGCTGTTTTCCCATCCAT	GCCATGTTCTATCGGGTACTTC
SIRT1	GCAGATTAGTAGGCGGCTTG	GCTGGTGGAACAATTCCTGT
SIRT2	TGCGGAACTTATTCTCCCAGA	GAGAGCGAAAGTCGGGGAT
Sox9	AGCGAACGCACATCAAGAC	CTGTAGGCGATCTGTTGGGG
CD24	CTCCTACCCACGCAGATTTATTC	AGAGTGAGACCACGAAGAGAC
ERa	ATTTGAAGTGGGCATGAGAACAT	CAATACCAACATCAGCCAGAAA
ERBB3	CTGATCACCGGCCTCAAT	GGAAGACATTGAGCTTCTCTGG
GATA3	GCGGGCTCTATCACAAAATGA	GCTCTCCTGGCTGCAGACAGC
KRT18	TGATGACACCAATATCACACGAC	TACCTCCACGGTCAACCCA
KRT14	CATGAGTGTGGAAGCCGACAT	GCCTCTCAGGGCATTCATCTC
CD44	AGATCAGTCACAGACCTGCC	GCAAACTGCAAGAATCAAAGCC
ALDH3	TGTGCGGACGCTGACTTGGAC	GGCATACTCCACGCTCCGCC
BMI1	AGCCATTTTGATTGCTGTTTGA	CCGCTTTTAGGCATACAGATTGTA
CD34	CAACACCTAGTACCCTTGGAAGT	ACTGTCGTTTCTGTGATGTTTGT
VIM	GAGTCCACTGAGTACCGGAGAC	TGTAGGTGGCAATCTCAATGTC
GAPDH	GAGTCAACGGATTTGGTCGT	TTGATTTTGGAGGGATCTCG

SUPPLEMENTAL REFERENCES

Cerami, E, Gao, J, Dogrusoz, U, Gross, BE, and Sumer, SO (2012). The cBio cancer genomics portal: an open platform for exploring multidimensional cancer genomics data. Cancer Discovery.

Gao, J, Aksoy, BA, Dogrusoz, U, and Dresdner, G (2013). Integrative analysis of complex cancer genomics and clinical profiles using the cBioPortal. Science.

Koboldt, D.C., Fulton, R.S., McLellan, M.D., Schmidt, H., Kalicki-Veizer, J., McMichael, J.F., Fulton, L.L., Dooling, D.J., Ding, L., and Mardis, E.R. (2012). Comprehensive molecular portraits of human breast tumours. Nature *490*, 61–70.

Phillips, S., Prat, A., Sedic, M., Proia, T., Wronski, A., Mazumdar, S., Skibinski, A., Shirley, S.H., Perou, C.M., Gill, G., et al. (2014). Cell-state transitions regulated by SLUG are critical for tissue regeneration and tumor initiation. Stem Cell Reports *2*, 633–647.

Van ’t Veer, L.J., Dai, H., van de Vijver, M.J., He, Y.D., Hart, A.A., Mao, M., Peterse, H.L., van der Kooy, K., Marton, M.J., Witteveen, A.T., et al. (2002). Gene expression profiling predicts clinical outcome of breast cancer. Nature *415*, 530–536.